The Astrophysical Journal, 640:L139–L142, 2006 April 1

SHALLOW DECAY OF EARLY X-RAY AFTERGLOWS FROM INHOMOGENEOUS GAMMA-RAY BURST JETS

Kenji Toma,[1] Kunihito Ioka,[1] Ryo Yamazaki,[2] and Takashi Nakamura[1]
Received 2005 November 25; accepted 2006 February 15; published 2006 March 8

ABSTRACT

Almost all the X-ray afterglows of γ-ray bursts (GRBs) observed by the *Swift* satellite have a shallow decay phase in their first few thousand seconds. We show that in an inhomogeneous-jet model (multiple-subjet or patchy-shell), the superposition of the afterglows of off-axis subjets (patchy shells) can produce the shallow decay phase. The necessary condition for obtaining the shallow decay phase is that γ-ray–bright subjets (patchy shells) have γ-ray efficiencies higher than previously estimated and that they be surrounded by γ-ray–dim subjets (patchy shells) with low γ-ray efficiency. Our model predicts that events with dim prompt emission will have a conventional afterglow light curve without a shallow decay phase, like GRB 050416A.

Subject headings: gamma rays: bursts — gamma rays: theory

1. INTRODUCTION

Before the *Swift* era, most X-ray and optical afterglows from γ-ray bursts (GRBs) were detected only several hours after the burst trigger. *Swift* observations are now unveiling the first several hours of the afterglows (see, e.g., Tagliaferri et al. 2005; Chincarini et al. 2005; Nousek et al. 2006; Cusumano et al. 2006; Hill et al. 2006; Vaughan et al. 2006). Recently, Nousek et al. (2006) analyzed the first 27 afterglows detected by the *Swift* X-Ray Telescope (XRT) and reported that almost all the early X-ray afterglows of *Swift* GRBs fail to show a simple power-law flux decline. They instead exhibit a "canonical" behavior in which the light curve begins with a very steep decay, which turns into a very shallow decay $\sim t^{-0.5}$ and finally connects to the conventional late-phase afterglow $\sim t^{-1}$, similar to what was observed in the pre-*Swift* era.

The shallow decay phase implies that more time-integrated radiation energy is observed at later times. This is unexpected in the standard model to explain the late-phase afterglows, that is, the synchrotron shock model for an impulsive homogeneous jet (for reviews, see Zhang & Mészáros 2004; Piran 2004). There seems to be essentially no spectral variation at the transition from the shallow decay phase to the conventional decay phase. This suggests that the origin of the transition is either hydrodynamic or geometric.

In the hydrodynamic model, the GRB jet is not impulsive, and the energy is injected continuously into the blast wave (Zhang et al. 2006; Nousek et al. 2006; Panaitescu et al. 2006; Granot & Kumar 2006; references therein). Such a continuous injection can be realized with either a long-lived central engine or a combination of a short-lived central engine with some distribution of the Lorentz factors of the launched shells. In the case of a long-lived central engine, more time-integrated injected energy is required at later times, while the injection should be stopped abruptly at some point ($\sim 10^4$ s). For a short-lived central engine, slower shells should have more energy than faster ones, and a lower cutoff should exist for the Lorentz factor. Since afterglows are dim in the shallow decay phase, the γ-ray efficiency for the front shells is much higher than previously estimated, both in the long-lived central engine case and in the short-lived central engine case. This is problematic in the framework of the internal-shock model.

In the geometric model, it is assumed that we observe more energetic regions of the GRB jet at later times as the afterglow shock decelerates and the visible region increases. The shallow decay phase of the "canonical" afterglow may be a combination of the tail of the prompt emission and delayed afterglow emission from an off-axis jet (Eichler & Granot 2006). In this picture, the duration and the flatness of the shallow decay phase correlate with the spectral peak photon energy E_p and the isotropic γ-ray energy $E_{\gamma,\mathrm{iso}}$, because all these quantities depend on the viewing angle. The jet break occurs just after the off-axis afterglow is observed, so the conventional decay phase ($\sim t^{-1}$) is expected to be short. Since Eichler & Granot (2006) discussed a specific "ring-shaped" jet, more general studies of the jet angular structure are desirable to elucidate the general characteristics of the geometric model (see also Panaitescu et al. 2006).

In this Letter, we develop an inhomogeneous-jet model to reproduce the "canonical" X-ray afterglows of GRBs in the framework of the geometric model. In order to study the angular energy distribution in the jet, we consider an extremely inhomogeneous jet (a multiple-subjet model). Figure 1 illustrates the setup for our analysis of an inhomogeneous jet. We assume that the whole jet (*dashed circle*) consists of multiple subjets (*solid circles*) and that the energy injected between subjets is negligible compared with the energy inside each subjet. Each subjet is assumed to generate prompt γ-ray radiation and a subsequent afterglow following the standard scenario. We calculate the early phase of the afterglow by superposing the contribution of each subjet and study the conditions necessary to reproduce the "canonical" afterglows of the *Swift* GRBs.

Inhomogeneous-jet models have been used to study the diversity of the prompt emission of GRBs (Nakamura 2000; Kumar & Piran 2000). The geometric effects in such models can explain the Amati correlation (Toma et al. 2005; Eichler & Levinson 2004; Yamazaki et al. 2004) and even the Ghirlanda correlation (Levinson & Eichler 2005). The patchy-shell model has also been used to explain the observed variability of the early afterglow light curve and the polarization of particular events, such as GRB 021004 (e.g., Nakar & Oren 2004).

In § 2, we study the necessary conditions for the jet properties to reproduce the "canonical" afterglows. A summary and discussion are given in § 3.

[1] Department of Physics, Kyoto University, Kitashirakawa, Sakyo-ku, Kyoto 606-8502, Japan; toma@tap.scphys.kyoto-u.ac.jp.
[2] Department of Physical Science, Hiroshima University, 1-3-1 Kagamiyama, Higashi-Hiroshima 739-8526, Japan.

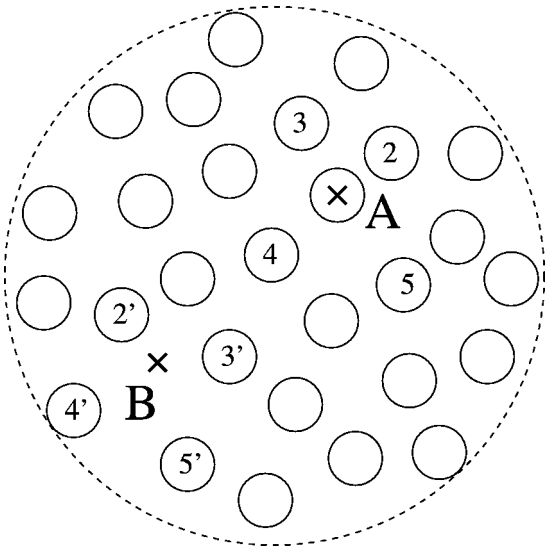

FIG. 1.—Setup for our analysis of an inhomogeneous jet. The whole jet (*dashed circle*) consists of multiple subjets (*solid circles*). Points "A" and "B" describe the lines of sight for our calculations. We take the initial opening half-angle of the subjets and the whole jet as $\Delta\theta_0^i = 0.01$ rad and $\Delta\theta_0^w = 0.1$ rad, respectively. Subjets 2, 3, 4, and 5 for line of sight A (similarly, 2′, 3′, 4′, and 5′ for line of sight B) have viewing angles θ_v^i of 0.025, 0.03, 0.035, and 0.04 rad.

2. NECESSARY CONDITIONS FOR THE SHALLOW DECAY OF EARLY X-RAY AFTERGLOWS

Figure 1 shows an example of the initial jet structure. We may consider the initial opening half-angle of each subjet $\Delta\theta_0^i$ to be $\gtrsim\Gamma_0^{i-1}$, where $\Gamma_0^i \simeq 10^2$–10^3 is the initial Lorentz factor of each subjet. The superscripts *i* and *w* denote each subjet and the whole jet, respectively, while the subscript 0 denotes the initial time when each subjet begins to decelerate. Each subjet is assumed to emit the prompt emission by virtue of the internal shock and the subsequent afterglow by synchrotron emission from the external shock of an impulsive homogeneous jet. We assume that all the subjets are ejected at essentially the same time, that is, over a period that is much shorter than the timescale of the afterglow.

In the following, we discuss the necessary conditions to explain the "canonical" behavior of the X-ray afterglows of *Swift* GRBs. The discussion is separated into two cases: In case 1, the line of sight is along a subjet. In case 2, the line of sight is off-axis for every subjet. For both cases we will obtain the conditions necessary to reproduce the "canonical" afterglow.

2.1. *Case 1*

In this case the line of sight is, for example, "A" in Figure 1. The shaded band in Figure 2 shows the afterglow light curve in the 2–10 keV range obtained in our calculation. This demonstrates that in case 1 a "canonical" afterglow light curve can be obtained, under certain conditions explained below.

We follow Panaitescu & Kumar (2001) in calculating the X-ray afterglow emission from an external shock due to an impulsive homogeneous jet with a sharp edge. The jet dynamics is calculated from the mass and energy conservation equations including the effect of sideways expansion at the local sound speed and radiative energy losses. The initial radius of the shell is set to be 0.01 times the deceleration radius. For the calculation of the synchrotron emission, the spectrum is approximated as a piecewise power law with injection break ν_m and cooling break ν_c. We neglect the self-absorption break because we focus on the spectrum for $\nu > \min(\nu_m, \nu_c)$. The received flux is calculated by integrating over the equal–arrival-time surface of photons to the observer. Neither synchrotron self-Compton emission nor reverse-shock emission is taken into account, for simplicity. In all the following calculations, we fix the initial Lorentz factor of the shell as $\Gamma_0 = 300$, the initial opening half-angle of the subjets as $\Delta\theta_0^i = 0.01$ rad, the number density of the circumburst medium as $n = 1\ \mathrm{cm}^{-3}$, the ratio of the magnetic energy and the accelerated electron energy to the shocked thermal energy as $\epsilon_B = 0.01$ and $\epsilon_e = 0.1$, respectively, and the index of the energy distribution function of the accelerated electrons as $p = 2.3$.

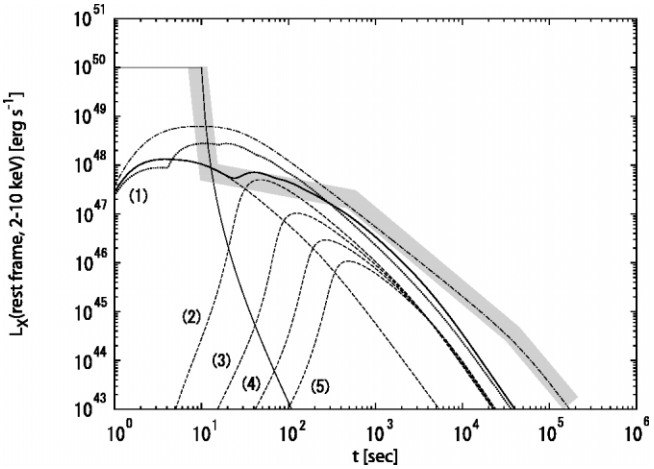

FIG. 2.—Example of the afterglow light curve (isotropic-equivalent luminosity) in the 2–10 keV range, measured in the cosmological rest frame of the GRB. The dot-dashed line is the afterglow from a jet with $E_{k,\mathrm{iso}}^w = 10^{52}$ ergs, $\Delta\theta_0^w = 0.1$ rad, and $\theta_v = 0$. The thin horizontal line ($t < 10$ s) represents a typical prompt burst that corresponds to the late phase of the (dot-dashed line) afterglow. The thin solid curve that continues for $t > 10$ s represents the tail of the prompt emission, which we set proportional to $(t - 9.0)^{-3.5}$. The dashed line labeled "1" is the afterglow from a subjet with $E_{k,\mathrm{iso}}^i = 3 \times 10^{51}$ ergs, $\Delta\theta_0^i = 0.01$ rad, and $\theta_v^i = 0$. Dashed lines 2, 3, 4, and 5 are the afterglows from subjets with $E_{k,\mathrm{iso}}^i = 3 \times 10^{52}$ ergs, $\Delta\theta_0^i = 0.01$ rad, and θ_v^i of 0.025, 0.03, 0.035, and 0.045 rad, respectively. These correspond to subjets 2, 3, 4, and 5 for line of sight A (or 2′, 3′, 4′, and 5′ for line of sight B) in Fig. 1. The thick solid line is the superposition of dashed lines 1–5. The shaded band is what we expect for the afterglows from inhomogeneous GRB jets. The dotted line is described in § 3.

In Figure 2, the dot-dashed line represents the afterglow light curve expected prior to the *Swift* era, that is, the afterglow from a homogeneous jet with a typical afterglow energy $E_{k,\mathrm{iso}}^w = 10^{52}$ ergs, an opening half-angle of $\Delta\theta_0^w = 0.1$ rad, and a viewing angle of $\theta_v = 0$. The X-ray afterglow emission has a rising light curve peaking at the shell deceleration time $t_{\mathrm{dec}} \simeq 5[E_{k,\mathrm{iso}}^w/(10^{52}\ \mathrm{ergs})]^{1/3}(\Gamma_0/300)^{-8/3}n^{-1/3}$ s. Around this time the XRT band is crossed by ν_m and ν_c for typical parameters (Sari et al. 1998), so that after the peak the light curve shows a smooth decline of $\sim t^{-1.2}$. The jet break time is estimated as $t_{\mathrm{jet}}^w \simeq 2 \times 10^4[\Delta\theta_0^w/(0.1\ \mathrm{rad})]^{8/3}[E_{k,\mathrm{iso}}^w/(10^{52}\ \mathrm{ergs})]^{1/3}n^{-1/3}$ s (Sari et al. 1999). After this time the light curve steepens to $\sim t^{-2.3}$, although the steepening is gradual (see Kumar & Panaitescu 2000).

The thin horizontal line around $L_X \sim 10^{50}$ ergs s^{-1} and for $t < 10$ s represents a typical prompt burst with a duration of $\simeq$10 s. The isotropic X-ray energy is about $\sim 10^{51}$ ergs, and for the typical GRB spectrum $\nu F_\nu \propto \nu$ at low energy, the isotropic

γ-ray energy should be about $\gtrsim 10^{52}$ ergs. This is comparable to or larger than the afterglow energy $E^w_{k,\rm iso} = 10^{52}$ ergs seen in actual observations (Lloyd-Ronning & Zhang 2004). The thin solid curve for $t > 10$ s is the tail part of the prompt burst, which comes from the regions of the jet at large viewing angles. The temporal index of the tail can be approximated as roughly $-1 + \beta$, where $\beta \sim -2.5$ is the high-energy photon index of the prompt emission (e.g., Zhang et al. 2006). Even if the emission regions are quite patchy, the tail emission may be smooth, since pulses from large viewing angles are of long duration and overlap with each other (Yamazaki et al. 2005).

First, consider the on-axis subjet that includes line of sight A in Figure 1. If the afterglow energy of the on-axis subjet is as large as $E^i_{k,\rm iso} = 10^{52}$ ergs, the afterglow flux is comparable to that shown by the dot-dashed line. Then it overwhelms the tail part of the prompt emission, and the temporal index of the afterglow emission just after the prompt burst will be $\sim t^{-1.2}$ or $\sim t^{-2.3}$, which is inconsistent with the steep decay observed by XRT. The dashed line labeled "1" in Figure 2 is the afterglow emission from the on-axis subjet, with $E^i_{k,\rm iso} = 3 \times 10^{51}$ ergs. Compared with the dot-dashed line (afterglow), with $E^w_{k,\rm iso} = 10^{52}$ ergs, we see that the deceleration time $t_{\rm dec}$ is a little earlier and the peak luminosity is smaller, since the spectral peak flux is $F_{\nu,\rm max} \propto E_{k,\rm iso}$. The jet break time of the subjet is much smaller because of the strong dependence of $t^i_{\rm jet}$ on $\Delta\theta^i_0$ and is estimated as $t^i_{\rm jet} \simeq 30[\Delta\theta^i_0/(0.01\ {\rm rad})]^{8/3}[E^i_{k,\rm iso}/(3 \times 10^{51}\ {\rm ergs})]^{1/3} n^{-1/3}$ s. In this case the steep decay due to the tail of the prompt emission can be observed. Therefore, the afterglow energy $E^i_{k,\rm iso}$ of the on-axis subjet should be at most one-third of that of the dot-dashed line, which is typical of the pre-*Swift* era.

Secondly, we can show that the shallow afterglow can be produced by the superposition of the subjet emissions. In Figure 2 we show the afterglow emission from the off-axis subjets, which do not include line of sight A. The dashed lines 2, 3, 4, and 5 illustrate the afterglow emissions from the subjets with θ^i_v of 0.025, 0.03, 0.035, and 0.04 rad, respectively. These subjets are illustrated in Figure 1 and have equal afterglow energies $E^i_{k,\rm iso} = 3 \times 10^{52}$ ergs. This is larger than that of the dot-dashed line by a factor of 3. The time at the peak is when the emission from the edge of the subjet arrives at the observer and is larger for the subjet with larger θ^i_v (Granot et al. 2002). The superposed light curve of the on-axis and off-axis subjets is shown by the thick solid line, which displays a shallow decline compared with the conventional $\sim t^{-1.2}$ decline. If all the off-axis subjets have equal viewing angles, the superposition of their contributions produces a bump in our calculation. The real afterglow may nevertheless be flat, because two-dimensional hydrodynamic simulations show that the rising part of the light curve when viewed at $\Delta\theta^i_0 \lesssim \theta^i_v \lesssim 2\Delta\theta^i_0$ is much flatter than in one-dimensional calculations such as ours (Granot et al. 2002).

All the subjets expand sideways and then begin to merge with each other. They will cease to expand sideways because of their pressure and finally merge into one shell, producing the conventional afterglow emission. Although we cannot follow the merger process with our simple calculations, the merged whole jet would produce the conventional decline of the dot-dashed line at late times, since the average of the $E^i_{k,\rm iso}$ over the solid angle is similar to $E^w_{k,\rm iso} = 10^{52}$ ergs. Therefore we suppose that the shallow decay phase would smoothly connect to the dot-dashed line and the final afterglow would follow the shaded band in Figure 2.

The prompt emission is dominated by that from the on-axis subjet because of the beaming effect. Thus, the prompt burst energy $E^i_{\gamma,\rm iso}$ of the on-axis subjet is $\gtrsim 10^{52}$ ergs. Since $E^i_{k,\rm iso} \sim 3 \times 10^{51}$ ergs, this implies that the γ-ray efficiency for the on-axis subjet is $\epsilon_\gamma \equiv E^i_{\gamma,\rm iso}/(E^i_{\gamma,\rm iso} + E^i_{k,\rm iso}) \gtrsim 75\%$, which is larger than previously estimated. This requirement is similar to that from hydrodynamic models for the shallow decay afterglows.

Now, what is observed when our line of sight is along the subjet with an energetic afterglow of $E^i_{k,\rm iso} = 3 \times 10^{52}$ ergs? Let us assume that the "canonical" afterglow is also observed in this case. Then the energy of the prompt emission should be $E_{\gamma,\rm iso} \gtrsim 10^{53}$ ergs in order for the tail emission to be larger than the afterglow emission from the on-axis subjet. From the necessary condition for the shallow decay phase obtained in the above discussion, the number of energetic afterglow subjets should be larger than that of the high γ-ray efficiency subjets. This leads to a larger rate of more energetic prompt bursts, which is not consistent with current observations. Therefore, the subjets with energetic afterglows should have low γ-ray efficiency and dim prompt emission, so that they are hard to observe.

In summary, a subjet that creates a bright prompt burst should have a dim afterglow and be surrounded by several subjets with dim prompt bursts and bright afterglows. A favorable GRB jet may have discrete spots with bright bursts and dim afterglows surrounded by such regions with dim bursts and bright afterglows.

2.2. *Case 2*

Next we consider the necessary conditions for a "canonical" afterglow to be observed when our line of sight is off-axis for every subjet, like "B" in Figure 1. The canonical afterglow light curve is obtained by the same calculation as in case 1, removing the contribution from the on-axis subjet. The afterglow light curves from subjets 2′, 3′, 4′, and 5′ in Figure 1 are the same as the dashed lines 2, 3, 4, and 5 in Figure 2, respectively. The nearest subjet (2′) should have a viewing angle of $\theta_{v,\rm min} \sim 2\Delta\theta^i_0$, because if $\theta^i_v < \theta_{v,\rm min}$ the contribution of the afterglow emission overwhelms the tail part of the prompt emission, while if $\theta^i_v > \theta_{v,\rm min}$ a rising afterglow appears after the tail of the prompt emission. The predicted total afterglow light curve in this case 2 is similar to that in case 1, that is, the shaded band.

In case 2 the γ-ray efficiency ϵ_γ should also be large. The prompt emission is dominated by the subjets with viewing angles $\theta^i_v \sim \theta_{v,\rm min}$. If the velocity of a point source makes an angle θ to the line of sight, the observed energy from this source will be proportional to $(1 - \beta\cos\theta)^{-3}$ because of the beaming effect. The observed energy from widely distributed segments of size $\Delta\theta^i_0$ with similar viewing angles θ^i_0 roughly follows $E_{\gamma,\rm iso} \propto [1 - \beta^i_0 \cos(\theta_{v,\rm min} - \Delta\theta^i_0)]^{-2}$ (Toma et al. 2005; Eichler & Levinson 2004; Levinson & Eichler 2005). This is derived by integration of the contribution of the point source over the solid angle occupied by the emission regions. Thus, in this case with $\theta_{v,\rm min} \sim 2\Delta\theta^i_0$, we receive a prompt burst energy $E_{\gamma,\rm iso} \sim (1 - \beta^i_0 \cos\Delta\theta^i_0)^{-2} E^i_{\gamma,\rm iso} \simeq (\Gamma^i_0 \Delta\theta^i_0)^{-4} E^i_{\gamma,\rm iso}$, where $E^i_{\gamma,\rm iso}$ is the isotropic energy of the prompt emission when a subjet is viewed on-axis. The received prompt energy is $E_{\gamma,\rm iso} \gtrsim 10^{52}$ ergs in the above calculation, and thus $E^i_{\gamma,\rm iso} \gtrsim 10^{54}$ ergs. Since $E^i_{k,\rm iso} = 3 \times 10^{52}$ ergs, we obtain $\epsilon_\gamma \gtrsim 97\%$. If this case predominates over case 1, we should observe many very bright GRBs when the line of sight is along the γ-ray–bright subjet. Thus, the con-

tribution of this case to the shallow decay afterglows would be small.

3. DISCUSSION

We have investigated early X-ray afterglows of GRBs within inhomogeneous-jet models by using a multiple-subjet model. We find that several off-axis subjets can reproduce the shallow decay phase of the light curves observed by the *Swift* XRT. The shallow decay phase is produced by the superposition of the afterglows from off-axis subjets, and it connects to the conventional late-phase afterglow produced by the merged whole jet.

We claim that the shallow decay phase arises prior to the merging of the subjets. The shape of the early afterglow light curve thus depends sensitively on the assumed sideways expansion speed of the subjets. The sideways expansion speed of the jet is highly uncertain and has been debated by use of hydrodynamic calculations (e.g., Kumar & Granot 2003; Cannizzo et al. 2004). In this Letter, we have assumed that each subjet expands sideways at the local sound speed. In Figure 2 we also show an afterglow light curve (a superposition of the subjet 1–5 fluxes) calculated under the assumption that each subjet expands at the local light speed (*dotted line*). The fluxes from the off-axis subjets peak earlier, so that the shallow decay phase disappears. If the local expansion is varied from the sound speed to the light speed, the light curve varies smoothly from the thick solid line to the dotted one. For the local light-speed case, we can obtain the shallow decay phase if the subjets are distributed more sparsely, for example, with θ_v^j of 0.032, 0.037, 0.042, and 0.047 rad for the off-axis subjets. However, if each subjet makes a hot cocoon that expands relativistically in the laboratory frame, all the subjets would merge around the deceleration time and the light curve would be the conventional one, that is, the dot-dashed line in Figure 2.

We determined the necessary conditions to obtain a "canonical" afterglow by separating our discussions into two cases, that is, whether the line of sight is along a subjet (case 1) or not (case 2). In both cases, subjets producing bright prompt emission require γ-ray efficiencies larger than previously estimated. This requirement is similar to the hydrodynamic model (Zhang et al. 2006; Nousek et al. 2006) and is problematic in the framework of the internal-shock model.

There are some predictions from our model. First, in case 1, a subjet producing a bright prompt burst should have dim afterglow emission and should be surrounded by several subjets producing dim prompt yet bright afterglow emissions. The possibility of such a jet structure cannot be excluded at present and should be tested with future observations. When the line of sight is along the subjet with dim prompt and bright afterglow emission, the conventional afterglow light curve without a shallow phase is obtained. Therefore we predict that low-$E_{\gamma,\mathrm{iso}}$ events should have conventional afterglow light curves. Among 10 *Swift* GRBs with known redshifts, GRB 050416A has an extremely small $E_{\gamma,\mathrm{iso}}$ of $\lesssim 10^{51}$ ergs and does not have a shallow decay phase (Nousek et al. 2006). This event may support case 1 of our inhomogeneous-jet model, although more statistics are required in order to confirm the validity of the model. Secondly, the number of subjets with dim bursts and bright afterglows should be several times larger than that of the observed γ-ray–bright subjets. Thus the true GRB rate should be several times larger than current estimates. In addition, since many subjets are γ-ray–dark, the mean γ-ray efficiency over the whole jet does not need to be so large (Kumar & Piran 2000). Only a subjet that happens to emit almost all of its energy into γ-rays would be observed as a GRB.

Case 2 suggests that for most events both the prompt and the afterglow emission arise from off-axis viewing angles, similar to the scenario of Eichler & Granot (2006). In this case, we found that most of the subjets should produce bright prompt emission and dim afterglow emission. When the line of sight is along such a subjet, the conventional but dim afterglow is observed. Then, we predict, there should be large-$E_{\gamma,\mathrm{iso}}$ events with the conventional afterglow in case 2. We should observe such bright γ-ray events at a rate similar to that of the "canonical" events, which may be tested in future.

We thank G. Sato and T. Takahashi for useful discussions. This work was supported in part by a Grant-in-Aid for the 21st Century Center of Excellence "Center for Diversity and Universality in Physics" from the Ministry of Education, Culture, Sports, Science and Technology (MEXT) of Japan and also by Grants-in-Aid for Scientific Research from the Japanese Ministry of Education, Culture, Sports, Science, and Technology, Nos. 14047212 (K. I. and T. N.), 14204024 (K. I. and T. N.), and 17340075 (T. N.).

REFERENCES

Cannizzo, J. K., Gehrels, N., & Vishniac, E. T. 2004, ApJ, 601, 380
Chincarini, G., et al. 2005, ApJ, submitted (astro-ph/0506453)
Cusumano, G., et al. 2006, ApJ, 639, 316
Eichler, D., & Granot, J. 2006, ApJL, in press (astro-ph/0509857)
Eichler, D., & Levinson, A. 2004, ApJ, 614, L13
Granot, J., & Kumar, P. 2006, MNRAS, 366, L13
Granot, J., Panaitescu, A., Kumar, P., & Woosley, S. E. 2002, ApJ, 570, L61
Hill, J. E., et al. 2006, ApJ, 639, 303
Kumar, P., & Granot, J. 2003, ApJ, 591, 1075
Kumar, P., & Panaitescu, A. 2000, ApJ, 541, L9
Kumar, P., & Piran, T. 2000, ApJ, 535, 152
Levinson, A., & Eichler, D. 2005, ApJ, 629, L13
Lloyd-Ronning, N. M., & Zhang, B. 2004, ApJ, 613, 477
Nakamura, T. 2000, ApJ, 534, L159
Nakar, E., & Oren, Y. 2004, ApJ, 602, L97
Nousek, J. A., et al. 2006, ApJ, in press (astro-ph/0508332)
Panaitescu, A., & Kumar, P. 2001, ApJ, 554, 667
Panaitescu, A., Mészáros, P., Gehrels, N., Burrows, D., & Nousek, J. 2006, MNRAS, 366, 1357
Piran, T. 2004, Rev. Mod. Phys., 76, 1143
Sari, R., Piran, T., & Halpern, J. P. 1999, ApJ, 519, L17
Sari, R., Piran, T., & Narayan, R. 1998, ApJ, 497, L17
Tagliaferri, G., et al. 2005, Nature, 436, 985
Toma, K., Yamazaki, R., & Nakamura, T. 2005, ApJ, 635, 481
Vaughan, S., et al. 2006, ApJ, 638, 920
Yamazaki, R., Ioka, K., & Nakamura, T. 2004, ApJ, 606, L33
Yamazaki, R., Toma, K., Ioka, K., & Nakamura, T. 2005, MNRAS, submitted (astro-ph/0509159)
Zhang, B., Fan, Y. Z., Dyks, J., Kobayashi, S., Mészáros, P., Burrows, D. N., Nousek, J. A., & Gehrels, N. 2006, ApJ, in press (astro-ph/0508321)
Zhang, B., & Mészáros, P. 2004, Int. J. Mod. Phys. A, 19, 2385